Electronic Supplementary Material (ESI) for Journal of Materials Chemistry C.

Supporting Information

Multidirectional biomimetic deformation of microchannel programmed metal nanowires liquid crystal networks

Lanshan Zhang, Jingkai Pan, Chenxu Gong, Aimin Zhang*

Materials. 4-nitrobenzoic acid, sodium hydroxide, glucose (analytical grade), potassium carbonate, acetic acid, allyl bromide, N,N-dimethylformamide (DMF) and all analytical reagents were purchased from Aladdin. Unless otherwise stated, all reagents and solvents were used without further purification.

General characterizations. The UV absorption spectrum of azobenzene molecule (MAB) was measured using a UV-3600 spectrophotometer (Shimadzu). The ^{1}H NMR spectrum of MAB was collected to confirm the molecular structure information by a Bruker-AVANCE III HD 400 nuclear magnetic resonance spectrometer (Bruker). $CDCl_3$ was used as reagent.

Synthesis of MAB. 4-Nitrobenzoic acid (7.5 g, 0.055 mol), NaOH (25.0 g, 0.625 mol) and deionized H_2O (120 mL) were mixed in a 500 mL round-bottom flask and stirred vigorously at 50 °C for 25 min, which was labeled as solution A. Glucose (50.0 g, 0.228 mol) was dissolved in 75 mL of H_2O, which was named to be solution B. Then, the solution B was added dropwise to the solution A and stirred for 30 min at 55 °C. After cooling to room temperature, the product could be precipitated out once the PH of solution was adjusted to 6 using 36 wt% acetic acid. The precipitation was washed at least three times with distilled water. The crude product was purified by 3 cycles of dissolution-precipitation processes using hot 10 wt% potassium carbonate solution and acetic acid. Finally, the product (AB) was washed with distilled water until the lotion became neutral, and then dried at 65 °C for 24 h. The dried product was dissolved in 200 ml of DMF, and an appropriate amount of 3-bromopropene was added. Then, the mixture was vigorously stirred at 90 °C for 24 h, and filtered after cooling. The desired MAB product was precipitated out by adding 600 mL of brine ice, and then filtered, washed and dried.

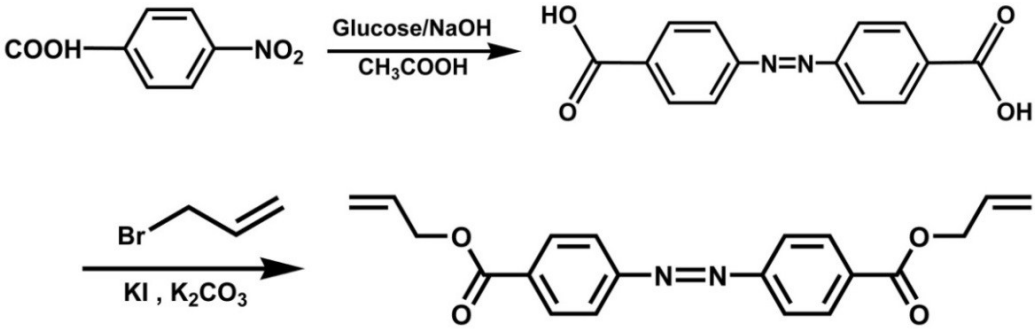

Fig. S1 Schematic diagram of the synthetic route of MAB

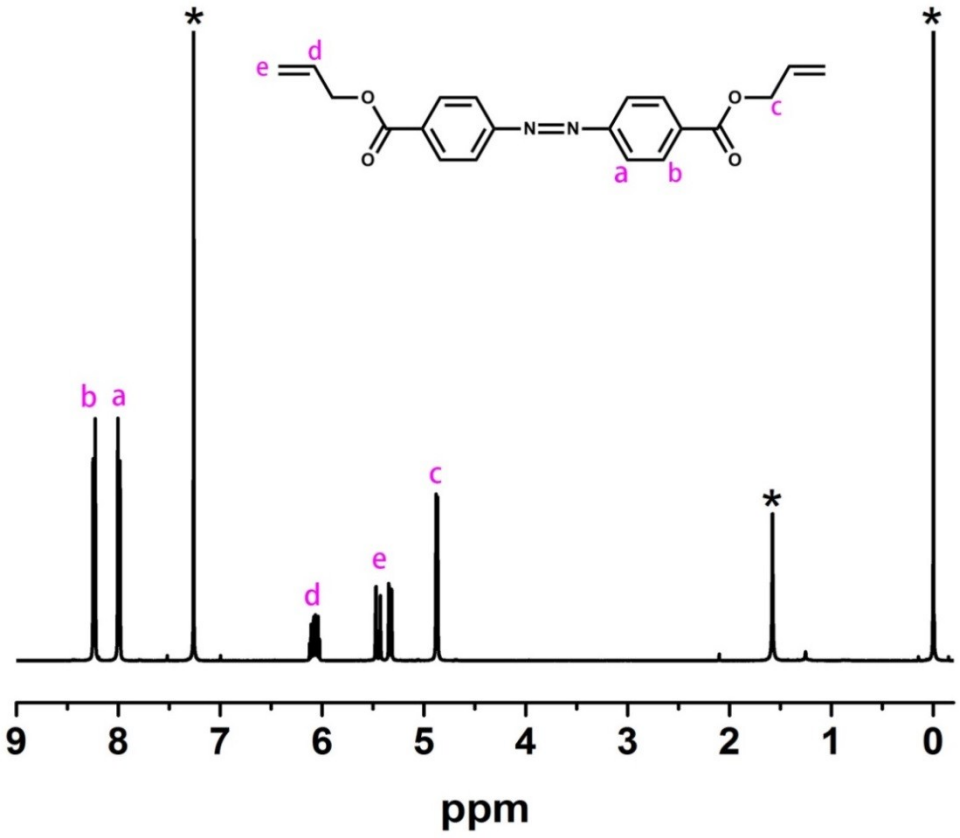

Fig. S2 ^{1}HNMR spectrum of MAB in $CDCl_3$

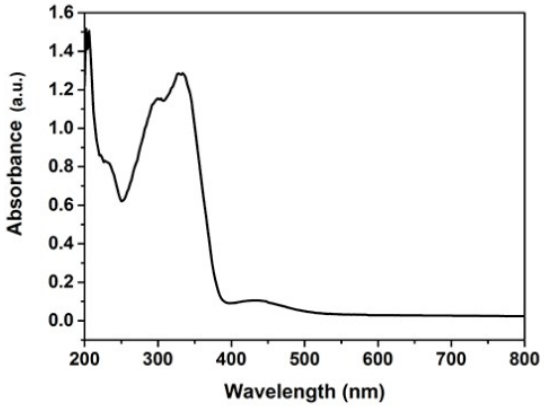

Fig. S3 UV-Vis spectrum of a solution of MAB in acetone.

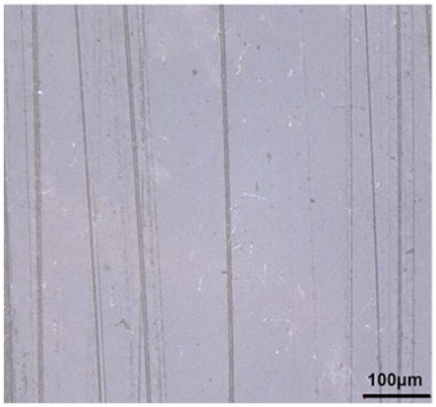

Fig. S4 Distribution of silver nanowires in film

As illustrated in Fig. S5, FTIR spectroscopy, which is rather sensitive to the groups change, can be used to characterize the chemical structure of the synthesized products. From Fig. S5, the wavenumber region of 3441 cm^{-1} is assigned to the vibration of -COOH. After the nucleophilic substitution reaction, the area of this region is significantly rdecreased. Further, the peaks at 1728 cm^{-1} and 1269 cm^{-1} can be attributed to the characteristic peaks of the ester group. The above results indicate the feasibility of nucleophilic substitution reaction in which the allyl group successfully replaces the hydrogen in the carboxyl group. The target product (MAB) was successfully synthesized.

According to the physico-chemical property of (4-[(4-carboxyphenyl)diazenyl]benzoic acid (AB) , its melting point is 360 °C. As can be seen from Fig. S6, the melting point of MAB is 113 °C, which is easier to melt and mix homogeneously with LC mixture(66°C).

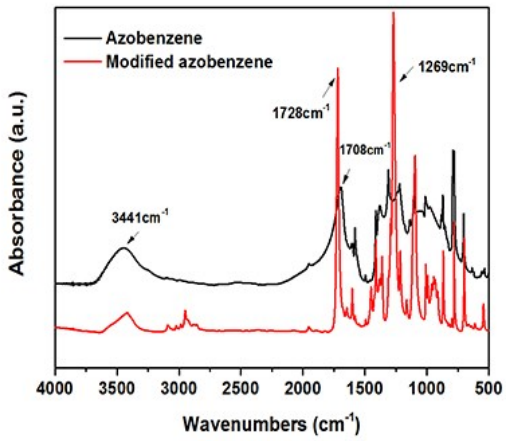

Fig. S5 FT-IR spectra of AB and MAB.

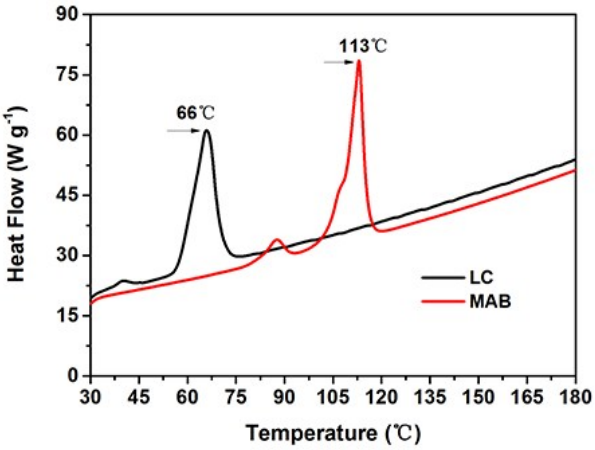

Fig. S6 DSC curves of MAB and LC mixture during a heating-cooling cycle (rate of 10 °C min^{-1}).

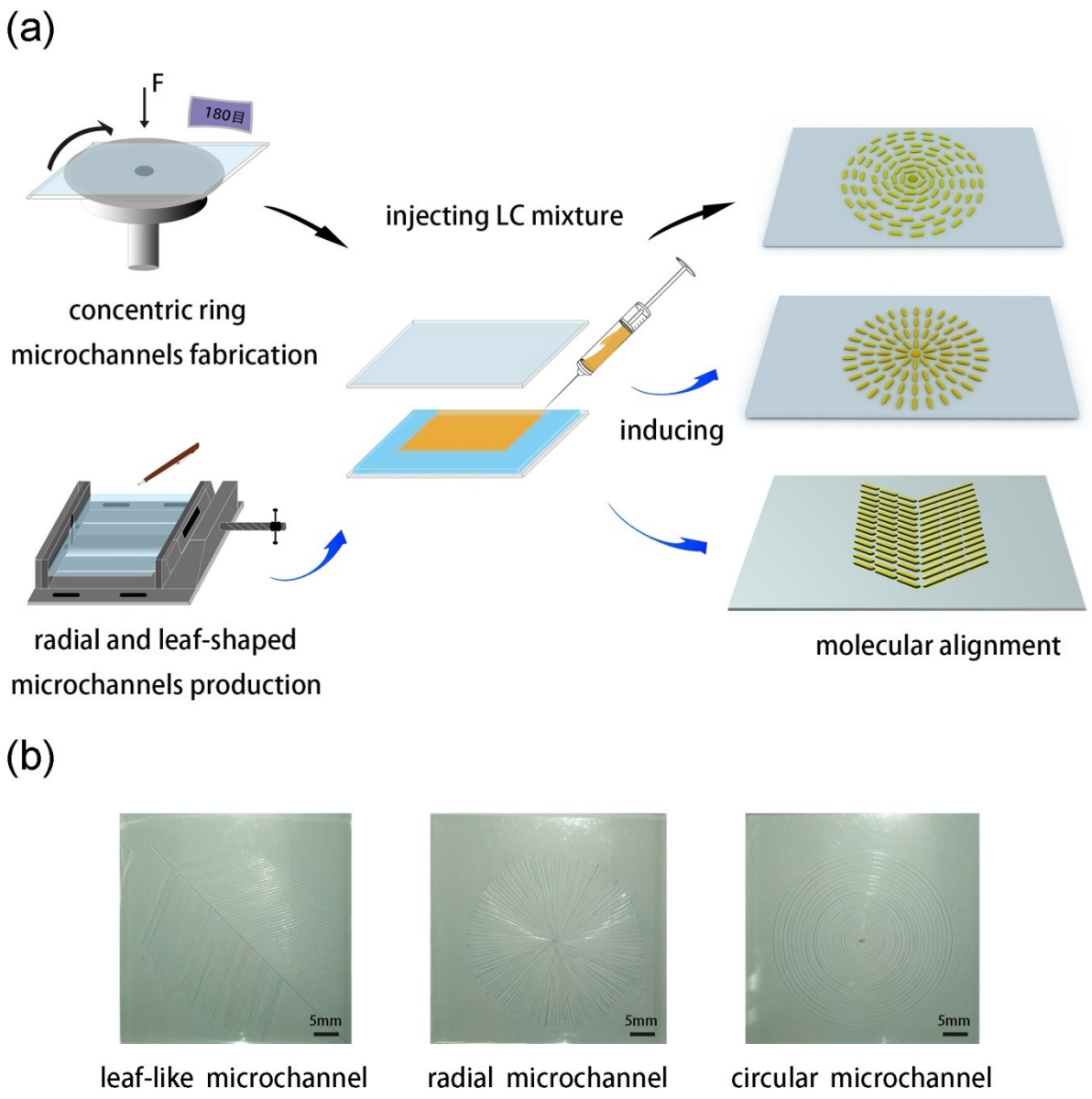

Fig. S7 Illustration of microchannel fabrication and the liquid crystal molecular alignment.

Details of microchannel fabrication

For the concentric ring microchannel fabrication, the glass substrate was placed on a rotating platform, and sandpaper was used to rub the glass plate under the vertical force. In addition, for the fabrication of radial and leaf-like microchannels, the glass substrate was fixed in the jig, and the microchannel structure was drawn by using diamond pen and ruler. Then the spacer strips was encapsulated with the glass substrate, leaving a gate to inject the LC mixture into the cell. As shown in Fig. S7, the molecules are arranged along the microchannels.

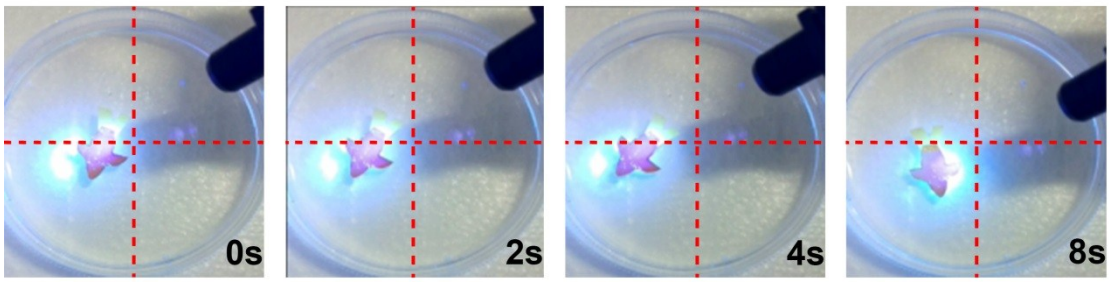

Fig. S8 The biomimic fish with AgNW-AZO/LCN tail and dye-doped PDMS body.

Table S1 Comparisons between the AgNW-AZO/LCN based actuator and previously reported photoresponse actuator.

Mechanism	Materials	Light source	Molecular orientation method	Bending angles	Recovery time	Reference
Photothermal effect and Photoisomerization effect	ALCE	365nm 550nm	Stretch orientation	N/A	30s	[1]
	AZO crosslink LCN	365nm 460nm	Stretch orientation	N/A	45s	[2]
	AZO doped LCE	470nm	Photo-alignment agent	300°	23s	[3]
	CLCP	365nm 530nm	mechanical rubbing	180°	14s	[4]
	AZO crosslink LCN	365nm	Stretch orientation	65°	N/A	[5]
	AZO doped LCE	488nm	Rubbing allignment Layer	90°	1s	[6]
	AZO doped LCE	532nm	Rubbing allignment Layer	90°	0.2s	[7]
	AZO doped LCE	365nm 660nm	Rubbing allignment Layer	70°	8s	[8]
	AgNW doped AZO-LCN	**365nm**	**Microchannel Inducing**	**170°**	**10s**	**This work**

Movie Captions.

Movie S1 The reversible bending process of the AgNW-AZO/LCN strip under 365 nm light (80 mW cm^{-2}) illumination.

Movie S2 Simulate the blooming/closing process of the Actuator-1.

Movie S3 The petals deformation and recovery of the Actuator-2 under UV irradiation.

Movie S4 The curling process of the smart biomimetic leaf (Actuator-3).

Movie S5 Light-controlled surfing of robotic swimmer based on AgNW doped LCN.

References

1. X. Lu, S. Guo, X. Tong, H. Xia and Y. Zhao, *Advanced materials*, 2017, **29**, 1606467.
2. M. Lahikainen, H. Zeng and A. Priimagi, *Nature communications*, 2018, **9**, 4148.
3. H. Zeng, O. M. Wani, P. Wasylczyk, R. Kaczmarek and A. Priimagi, *Advanced materials*, 2017, **29**, 1701814.
4. Y. Liu, B. Xu, S. Sun, J. Wei, L. Wu and Y. Yu, *Advanced materials*, 2017, **29**, 1604792.
5. A. H. Gelebart, M. Mc Bride, A. P. H. J. Schenning, C. N. Bowman and D. J. Broer, *Advanced Functional Materials*, 2016, **26**, 5322-5327.
6. O. M. Wani, H. Zeng and A. Priimagi, *Nature communications*, 2017, **8**, 15546.
7. D. Martella, S. Nocentini, D. Nuzhdin, C. Parmeggiani and D. S. Wiersma, *Advanced materials*, 2017, **29**, 1704047.
8. H. Zeng, P. Wasylczyk, C. Parmeggiani, D. Martella, M. Burresi and D. S. Wiersma, *Advanced materials*, 2015, **27**, 3883-3887.